

## SHAPE SENSITIVE INTENSITY FLUCTUATIONS USING STRUCTURED ILLUMINATION

Shubham DAWDA, Zhean SHEN and Aristide DOGARIU\*

CREOL, The College of Optics and Photonics, University of Central Florida, 4304 Scorpius Street, Orlando, Florida, 32816, USA.

\*Corresponding author: [adogariu@creol.ucf.edu](mailto:adogariu@creol.ucf.edu)

### Abstract

We describe the intensity fluctuations due to scattering from sparse distributions of axisymmetric dipolar particles illuminated by space-polarization entangled fields. We show that, unlike traditional type of illumination, this approach permits controlling the scattering regime and, in certain conditions, provides means to optimize the retrieval of asymmetry factors using the scattered intensity measured by a single detector.

### 1 Introduction

Traditional techniques for particle characterization by light scattering are based on well-defined interaction volumes [1, 2]. However, space-polarization entangled fields allow changing this paradigm and divide the interaction volume into distinct regions illuminated with different polarization states [3, 4]. Further, it is known that a polarimetric analysis of scattered fluctuations enables a more detailed characterization of random media [5]. In this work, we study the light scattering from a sparse group of anisotropic but axisymmetric particles illuminated by such a structured field and demonstrate that the contrast of intensity fluctuations is highly sensitive to particle anisotropy. The concepts and results of this work should be of interest for remote sensing and the characterization of particulate matter.

### 2 Scattering from 2 axisymmetric dipoles

The anisotropic polarizability of a single scattering object can be obtained by analyzing the statistical moments of polarimetrically measured intensity distributions [6, 7]. Here we start by examining the canonical example of two identical axisymmetric dipoles that are coherently excited. The particle's polarizability tensor is a diagonal matrix  $\alpha = \text{diag}(\alpha_1, \alpha_2, \alpha_2)$  characterized by the aspect ratio  $r = \frac{\alpha_1}{\alpha_2}$ . These scattering centers are at different but fixed spatial locations. Their orientations are independent of each other and are uniformly randomly distributed during the measurement. Let  $E_1$  and  $E_2$  be the projections of the fields scattered from each dipole onto a common polarization state. It can be shown that the first and second moments of the far-field scattered intensity,  $I = E^2 = (E_1 + E_2)^2$ , are

$$\begin{aligned} \langle I \rangle_o &= \langle E_1^2 \rangle_o + \langle E_2^2 \rangle_o + 2\langle E_1 \rangle_o \langle E_2 \rangle_o \\ \langle I^2 \rangle_o &= \langle E_1^4 \rangle_o + \langle E_2^4 \rangle_o + 6\langle E_1^2 \rangle_o \langle E_2^2 \rangle_o + \\ & 4\langle E_1^3 \rangle_o \langle E_2 \rangle_o + 4\langle E_1 \rangle_o \langle E_2^3 \rangle_o, \end{aligned} \quad (1)$$

where  $\langle \dots \rangle_o$  represents orientation averaging.

In the following, we will analyze the contrast  $C = \frac{\text{var}(I)}{\langle I \rangle_o^2}$  of intensity fluctuations for two types of illuminations shown in Figure 1. Each of the two dipoles can be excited by a field that is either parallel or orthogonal to the orientation of the analyzer generating "parallel"  $E_{\parallel}$  or "crossed"  $E_{\times}$  scattered fields, respectively. When both excitations are parallel to the analyzer orientation,  $\langle E_1^k \rangle_o = \langle E_2^k \rangle_o = \langle E_{\parallel}^k \rangle_o$  in Eq. (1) and the contrast can be written as

$$C_1 = \frac{\langle E_{\parallel}^4 \rangle_o + 3\langle E_{\parallel}^2 \rangle_o^2 + 4\langle E_{\parallel}^3 \rangle_o \langle E_{\parallel} \rangle_o}{2(\langle E_{\parallel}^2 \rangle_o + \langle E_{\parallel} \rangle_o^2)^2} - 1 \quad (2)$$

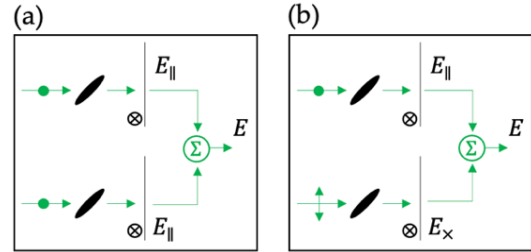


**Figure 1** Detected field  $E$  is generated by the coherent superposition of scattered fields from two independent dipoles, which are (a) both excited by field vectors parallel to analyzer orientation and (b) one of them is excited by field vector parallel and the other by a field orthogonal to the analyzer.

When one of the excitation fields is "crossed", it can be shown that  $\langle E_{\times} \rangle_o = \langle E_{\times}^3 \rangle_o = 0$  in Eq. (1) and the contrast becomes

$$C_2 = \frac{\langle E_{\parallel}^4 \rangle_o + \langle E_{\times}^4 \rangle_o + 6\langle E_{\parallel}^2 \rangle_o \langle E_{\times}^2 \rangle_o}{(\langle E_{\parallel}^2 \rangle_o + \langle E_{\times}^2 \rangle_o)^2} - 1. \quad (3)$$

Since the scatterers are axisymmetric, the contrasts will depend on their aspect ratio  $r$  ( $r > 1$  for prolate,  $r < 1$  for oblate, and  $r = 1$  for spherical particles). The two contrasts  $C_1$  and  $C_2$  are plotted in Figure 2 for the case where the dipoles are illuminated by equally intense fields. We note that, within a certain range of aspect ratios,  $\frac{dC_2}{dr} > \frac{dC_1}{dr}$ , which suggests that the statistical properties of the intensity fluctuations are more sensitive to shape when the excitation field are not both parallel to the analyzer's orientation.

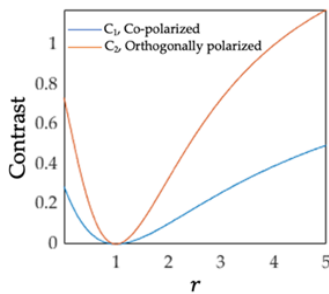


**Figure 2** Contrast of intensity fluctuations as function of aspect ratio when both excitation fields are parallel and when one of them is orthogonal to the direction of the analyser.

### 3 Scattering from group of axisymmetric particles

Let us now consider a more realistic situation where  $N$  identical axisymmetric randomly orienting dipolar particles are randomly positioned in space. The particle group is sufficiently sparse such that it scatters light in the so-called “single scattering” regime. Unlike the previous section, this process now is characterized by two stochastic parameters: random orientations and random positions.

When the particle group is excited by a space-polarization entangled field such as, for instance, a cylindrical vector beam, the total interaction volume can be considered as two distinct orthogonally polarized regions. Effectively, a fraction  $\nu \cdot N$  of all particles is excited by a field polarized parallel to the analyzer (co-polarized) and the rest of the particles are excited by a field polarized perpendicular to the analyzer (cross-polarized) as schematically shown in Figure 3.

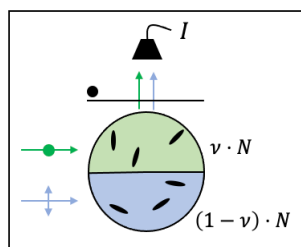


**Figure 3** Schematic of two spatially distinct and orthogonally polarized regions containing different numbers of identical, anisotropic, and randomly oriented particles.

When the final scattered field is modelled as a 2D random walk in the complex plane with distributed step lengths and uncorrelated particle positions and amplitudes [8, 9], the contrast is given by

$$C_{\parallel+\times} = 1 + \frac{1}{N} \left( \frac{\nu \left( \langle E_{\parallel}^4 \rangle_o - 2 \langle E_{\parallel}^2 \rangle_o^2 \right) + (1-\nu) \left( \langle E_{\times}^4 \rangle_o - 2 \langle E_{\times}^2 \rangle_o^2 \right)}{\left( \nu \langle E_{\parallel}^2 \rangle_o + (1-\nu) \langle E_{\times}^2 \rangle_o \right)^2} \right) \quad (4)$$

where  $E_{\parallel}$  and  $E_{\times}$  are scattered fields from a single dipole excited under co-polarized and cross-polarized conditions, respectively. In Eq. (4), setting  $\nu = 0$  and  $\nu = 1$  gives the contrast for the cross and co-polarized excitations of a single

interaction volume and setting  $\nu \in (0,1)$  gives the contrast for different volume ratios of orthogonally polarized interaction volume. These contrasts are plotted in Figure 4 as a function of aspect ratio for the case of  $N = 100$  particles.

There are three key features to note. First, in a cross-polarized setting ( $\nu = 0$ ), the contrast is independent of particle shape. Second, within a certain range of aspect ratios, the sensitivity of contrast to particle shape is higher for  $\nu < 1$  than that for  $\nu = 1$ . Third, the sensitivity of contrast is maximized when  $\nu$  is minimized.

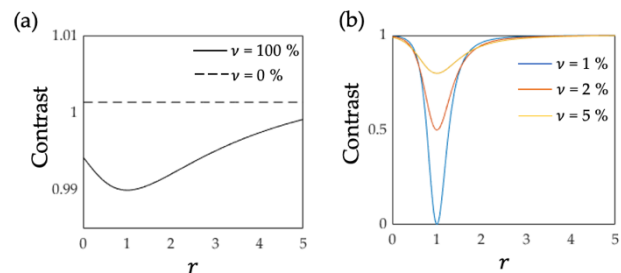


**Figure 4** Contrast of intensity fluctuations as a function of aspect ratio for 100 particles distributed (a) in a single co and cross-polarized and (b) two orthogonally polarized interaction volumes.

### 4 Discussion and Conclusions

The improved sensitivity can be understood by considering the length distributions and number of steps in the random walk model. Analyzing the orientation averaged scattered intensities indicates that when excited by identical fields, the intensity scattered by a single axisymmetric dipole is, on average, higher in the co-polarized setting. Hence, when a subset of all particles is excited in this manner, the magnitude of the associated phasors are increased compared to the ones corresponding to the cross-polarized particles. From a macroscopic point of view, the space-polarization structuring effectively reduces the total number of particles contributing to the final field leading to a non-gaussian distribution of measured intensities [8, 10].

Since the mismatch between co and cross-polarized scattered intensities reaches a maximum around  $r = 1$ , the effective number reduction is most prominent for particle aspect ratios close to 1. Consequently, the highest sensitivity enhancement is observed around  $r = 1$ , which could be an appealing practical characteristic. Furthermore, adjusting the volume ratio  $\nu$  allows control over the range of aspect ratios within which this improvement occurs.

In conclusion, we modeled the fluctuations of intensity scattered from a sparse distribution of subwavelength axisymmetric particles excited by space-polarization entangled fields. We demonstrate that by tuning the polarization state of the illumination across distinct spatial regions one can isolate the volume of interaction and effectively control the number of particles contributing to the detected intensity. This all-optical procedure permits establishing the desired regime of non-gaussian intensity

fluctuations in which the sensitivity to scatterers' asymmetry can be optimized. The results presented here should be of interest for characterizing non-spherical particles for biosensing[11, 12], monitoring polymerization[13, 14] and characterizing naturally occurring random media[15].

## 5 References

- [1] B. J. Berne and R. Pecora, *Dynamic light scattering: with applications to chemistry, biology, and physics*. Dover Publications, 2000.
- [2] J. G. Walker, P. C. Y. Chang, K. I. Hopcraft, and E. Mozaffari, "Independent particle size and shape estimation from polarization fluctuation spectroscopy," *Measurement Science and Technology*, vol. 15, no. 5, pp. 771-776, 2004/03/26 2004, doi: 10.1088/0957-0233/15/5/001.
- [3] Z. Bouchal and M. Olivik, "Non-diffractive Vector Bessel Beams," *Journal of Modern Optics*, vol. 42, no. 8, pp. 1555-1566, 1995/08/01 1995, doi: 10.1080/09500349514551361.
- [4] A. Aiello, F. Töppel, C. Marquardt, E. Giacobino, and G. Leuchs, "Quantum-like nonseparable structures in optical beams," *New Journal of Physics*, vol. 17, no. 4, p. 043024, 2015/04/15 2015, doi: 10.1088/1367-2630/17/4/043024.
- [5] *Photopolarimetry in Remote Sensing*. Kluwer Academic Publishers, 2004.
- [6] D. Haefner, S. Sukhov, and A. Dogariu, "Stochastic Scattering Polarimetry," *Physical Review Letters*, vol. 100, no. 4, p. 043901, 01/28/ 2008, doi: 10.1103/PhysRevLett.100.043901.
- [7] S. Sukhov, D. Haefner, and A. Dogariu, "Stochastic sensing of relative anisotropic polarizabilities," *Physical Review A*, vol. 77, no. 4, p. 043820, 04/16/ 2008, doi: 10.1103/PhysRevA.77.043820.
- [8] A. P. Bates, K. I. Hopcraft, and E. Jakeman, "Particle shape determination from polarization fluctuations of scattered radiation," *J. Opt. Soc. Am. A*, vol. 14, no. 12, pp. 3372-3378, 1997/12/01 1997, doi: 10.1364/JOSAA.14.003372.
- [9] E. Jakeman and K. D. Ridley, *Modeling Fluctuations in Scattered Waves*, 1 ed. CRC Press, 2006.
- [10] E. Jakeman, "Polarization characteristics of non-Gaussian scattering by small particles," *Waves in Random Media*, vol. 5, no. 4, pp. 427-442, 1995/10 1995, doi: 10.1088/0959-7174/5/4/004.
- [11] R. Chandrasekaran, T. Madheswaran, N. Tharmalingam, R. J. C. Bose, H. Park, and D.-H. Ha, "Labeling and tracking cells with gold nanoparticles," *Drug Discovery Today*, vol. 26, no. 1, pp. 94-105, 2021/01/01/ 2021, doi: <https://doi.org/10.1016/j.drudis.2020.10.020>.
- [12] X. Yang, M. Yang, B. Pang, M. Vara, and Y. Xia, "Gold Nanomaterials at Work in Biomedicine," *Chemical Reviews*, vol. 115, no. 19, pp. 10410-10488, 2015/10/14 2015, doi: 10.1021/acs.chemrev.5b00193.
- [13] R. Wu, J. R. Guzman-Sepulveda, A. P. Kalra, J. A. Tuszynski, and A. Dogariu, "Thermal hysteresis in microtubule assembly/disassembly dynamics: The aging-induced degradation of tubulin dimers," *Biochemistry and Biophysics Reports*, vol. 29, p. 101199, 2022/03/01/ 2022, doi: <https://doi.org/10.1016/j.bbrep.2021.101199>.
- [14] H. J.J. and J. T., "Online Monitoring of Polymerizations: Current Status," *European Journal of Organic Chemistry*, 2017.
- [15] P. Piedra, A. Kalume, E. Zubko, D. Mackowski, Y.-L. Pan, and G. Videen, "Particle-shape classification using light scattering: An exercise in deep learning," *Journal of Quantitative Spectroscopy and Radiative Transfer*, vol. 231, pp. 140-156, 2019/07/01/ 2019, doi: <https://doi.org/10.1016/j.jqsrt.2019.04.013>.